NJC

Accepted Manuscript

This is an *Accepted Manuscript*, which has been through the Royal Society of Chemistry peer review process and has been accepted for publication.

Accepted Manuscripts are published online shortly after acceptance, before technical editing, formatting and proof reading. Using this free service, authors can make their results available to the community, in citable form, before we publish the edited article. We will replace this *Accepted Manuscript* with the edited and formatted *Advance Article* as soon as it is available.

You can find more information about *Accepted Manuscripts* in the Information for Authors.

Please note that technical editing may introduce minor changes to the text and/or graphics, which may alter content. The journal's standard Terms & Conditions and the Ethical guidelines still apply. In no event shall the Royal Society of Chemistry be held responsible for any errors or omissions in this *Accepted Manuscript* or any consequences arising from the use of any information it contains.

ROYAL SOCIETY OF CHEMISTRY

www.rsc.org/njc

Cite this: DOI: 10.1039/c0xx00000x

www.rsc.org/xxxxxx

ARTICLE TYPE

Hydrothermal Treatment TiO_2 Film by Hydrochloric Acid for Efficient Dye-sensitized Solar Cells

Qiuxiang Wen, Jun Yu, Xiaoyong Sun, Jia Zhuang*, Quangui He, Xin You, Jiang Guo and Liying Tao

Received (in XXX, XXX) Xth XXXXXXXXX 20XX, Accepted Xth XXXXXXXXX 20XX
DOI: 10.1039/b000000x

The photovoltaic properties of nanoporous TiO_2 films treated by different concentrations hydrochloric acid (HCl), were investigated in Dye-sensitized Solar Cells (DSSCs). The nanostructure of the films were reformed, and their thickness were decreased after the HCl hydrothermal treatment via the SEM analysis. It had been found that the electron life time, band gap, recombination rate and electron injection efficiency of the TiO_2 films had been changed by the processing when different analysis methods were employed to analyze the experimental results, including OCVD, UV-Vis and Mott-Schottky plots. In addition, the schematic model of electron transfer and recombination had been showed to disscuss the processe more detailedly and clearly. The performances of the DSSCs based on the different TiO_2 films were measured by J-V curves and IPCE. When the TiO_2 film was treated by 1 mol Ł$^{-1}$ HCl at 180 ℃ for 3 h, the device had the optimum photo-electric conversion performance of 7.77 % and J_{sc} of 16.04 mA ċm^{-2}. The results suggested the reformed film's nanostructure leaded to the optimized electron transportion pathway, and the decreased electron recombination and increased injection efficiency resulted in the improvement of the DSSCs.

1. Introduction

Recent years, Dye-sensitized Solar Cells (DSSCs) was considered as the most potential solar energy conversion device for its advantages of low cost, low toxicity and excellent light permeability.[1,2] There were many oxides and multiple compounds acting as photoanode, such as TiO_2,[3-5] ZnO,[6,7] SnO_2,[8] Zn_2SnO_4 and $SrTiO_3$.[9,10] Among those materials, TiO_2 was the ideal choice because of the high energy level matching degree with dye and a better chemical stability.[11,12] At present, the nanocrystal TiO_2 nanoporous film is still the most promising structure for DSSCs photoanode. The advantage of nanocrystal TiO_2 nanoporous film comes from the high surface area which is beneficial to load more dye molecules and cause a high light harvesting. It is well-known that the light harvesting efficiency (LHE), the electron injection efficiency (η_{inj}) and the electron collection efficiency (η_{col}) are the leading factor to J_{sc} value.[13,14] However, there may not be fully interconnected between the particles and there are vacants when the nanoporous TiO_2 film had the networks structure.[15] It means that the electron from this part can not transport to the conductive glass successfully and the light harvesting efficiency (LHE) would be reduced.[16] Another part of electron losing comes from the recombination processes that occurs on the TiO_2 surface and the uncovered conductive glass surface with I_3^- in electrolyte.[17] And the electron injection efficiency (η_{inj}) is affected by the energy level relationship between the dye and titanium dioxide.[18]

A lot of work have been made to modify the TiO_2 nanoporous film for more efficiency solar energy conversion device, such as doping, surface treatment, construction of composite structure. Wide band gap metal oxide, insulator and co-adsorbing materials have been used to modify the TiO_2 nanoporous film, which were proven effective in improving the DSSCs conversion efficiency.[19-24] It has been demonstrated that the electron injection efficiency was increased and electron recombination reduced between conduction band and I_3^- in electrolyte when the nanoporous TiO_2 film was modified with 0.1M hydrochloric acid.[25] Jaspreet Singh treated nanoporous TiO_2 film with oxalic acid to obtain the improvement of short circuit density (J_{sc}) and open circuit voltage (V_{oc}) which resulting from the increased dye loading and efficient electron transfer.[26] Many other acids such as HNO_3, H_3PO_4, H_2SO_4, H_2O_2 have also been reported to improve the power conversion efficiency of the DSSCs.[27-30] Therefore, the surface treatment of TiO_2 film by various methods will effectively help to enhance the photo-electric conversion efficiency (PCE).

In this paper, the pre-prepared nanoporous TiO_2 films were treated by different concentrations hydrochloric acid (HCl) via hydrothermal method for the first time. The hydrothermal treated TiO_2 electrode was investigated and compared with the untreated TiO_2 electrode. The different structure of the hydrothermal treated TiO_2 electrodes and the corresponding performances of DSSCs have been reported and discussed.

2. Experimental

2.1 Preparation of TiO_2

First, anatase TiO_2 nanoparticles were prepared by hydrothermal method: 5 mL $TiCl_4$ was added into 45 mL deionized (DI) water containing 0.66g $(NH_4)_2SO_4$; the diluted ammonia was used to adjust the pH to 8 and water bath was used to heat the solution to 90 ℃ for 1 h under magnetic stirring; next, the precursor was transferred to Teflon-liner autoclaves which would be placed in an electric oven at 180 ℃ for 4 h to obtain the anatase TiO_2 nanoparticles. The FTO glasses were cleaned with water, ethanol and acetone by ultrasonic cleaning, respectively.

TiO_2 compact layer on the cleaned FTO substrate was prepared with 0.2 mol Ł$^{-1}$ $TiCl_4$ solution at 70 ℃ for 30 mim after been sintered in the air at 500 ℃ for 30 min. TiO_2 paste were prepared with 0.5g P25 and 0.5g anatase TiO_2 nanoparticles, 0.5g ethocel, 0.2 mL acetate and 4.3 mL terpineol. The nanoporous TiO_2 film was deposited by the doctor blade method on the pre-treatment FTO glass. After drying, the films were sintered via a typical sintering system. The pre-prepared nanoporous TiO_2 film was placed against the inside wall of Teflon-liner with the conductive side facing down. Different concentrations of hydrochloric acid were transferred to the teflon-lined autoclaves which would be placed in an electric oven at 180 ℃ for 3 h. When the temperature was down to 25 ℃, the sample was taken out and dried in the ambient air. Subsequently, the sample was sintered at 500 ℃ for 3 h. Finally, the sample was treated with 0.04 mol Ł$^{-1}$ $TiCl_4$ by the previous reported method.[32] The concentrations of hydrochloric acid were 0.5 mol Ł$^{-1}$, 1 mol Ł$^{-1}$, 2 mol Ł$^{-1}$, 3 mol Ł$^{-1}$, 4 mol Ł$^{-1}$ and the corresponding samples were named as 0.5HM, 1HM, 2HM, 3HM, 4HM, and the control film was named as CM.

2.2 Fabrication of the DSSC devices

The as-prepared films were immersed into N719 dye solution (0.3 mmol Ł$^{-1}$) at 25 ℃ for 24 h. The dye-sensitized films were washed with ethanol and dried at 40 ℃. The liquid electrolyte was high-efficiency electrolyte system (yingkou China, OPV tech new Energy Co, OPV-AN-I) and the platinum counter electrode (CE) was commercial product prepared with magnetron sputtering. The electrolyte of iodide/triiodide solution was added into the gap between the electrodes by an injector.

2.3 Characterization

The chemical composition of the films were examined by X-ray diffraction (XRD, DX-1000, Dandong, China) at a scanning speed of 3.6 °/min, and the morphologies were characterized by emission scanning electron microscopy (SEM, JSM-7500F, JEOL). The J-V curves and IPCE spectra were recorded with an electrochemical workstation under a simulated solar spectroscopy (AM1.5) produced by a solar simulator (CEL-S500, Beijing) and IPCE system (PVE 300) from 300 to 800 nm under the short-circuit conditions, respectively. Mott-Schottky measurements were based on three electrode systems that TiO_2 films were used as electrode, saturated calomel electrode (SCE) and Platinum electrode were served as reference electrode and counter electrode. The UV-vis absorption spectra of the film was measured on an UV−vis-NIR spectrophotometer (UV-1700, SHIMADZU). The active area of the solar cells was controlled to 0.25 cm^2 by a constant mask.

3. Result and discussion

3.1 Structure and morphology analysis of TiO_2 films

An insight into the phase and morphology of TiO_2 films were acquired through combing XRD analyses with SEM investigation of the top and section images. Fig.1 shows the XRD patterns of the control film (CM) and the samples treated with different concentrations of hydrochloric acid. The peak at 27 ° was the typical characteristic of SnO_2 oxide, which came from the FTO conductive substrate. The peak at 25 ° and 37 ° were the characteristic peaks belonging to anatase and rutile TiO_2, respectively. When the samples were treated by hydrothermal and sintering, the intensity of diffraction peaks at 25 ° were increased and FWHM values were reduced slightly which indicated the appearance of higher crystallinity and a increased grain size. It can be found that the sample of 1HM showed the optimal crystallinity when the treated TiO_2 films were compared furtherly.

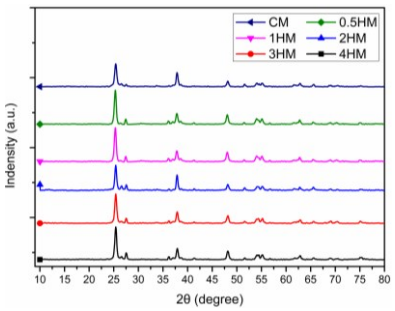

Fig.1 XRD patterns of TiO_2 films

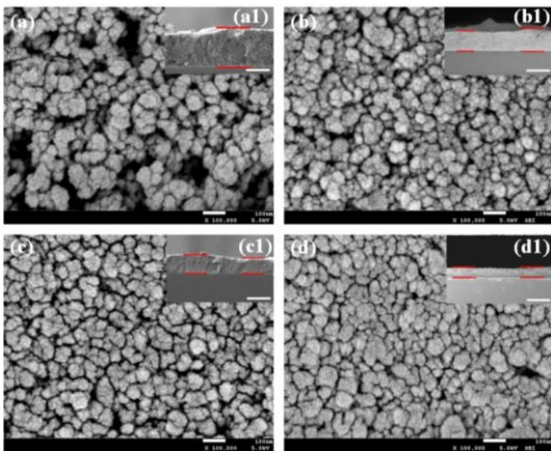

Fig.2 Top and section SEM images of the sample (a) CM, (b)1HM, (c) 2HM and (d) 4HM; the scale bar in the section image was 10 μm

Fig.2 shows the SEM images of the sample CM, 1HM, 2HM and 4HM. As shown in Fig.2(a), the TiO_2 nanoparticles were packed randomly, and the agglomeration of nanoparticles was existent with uneven distributed porosity. Then partial diameters of the apertures were more than 100nm which might lead to a rupture in the internal structure of TiO_2 film. The thickness of the sample CM was about 14.5 ± 0.5 μm which could be evaluated from Fig.2(a1). When the TiO_2 film was treated with 1 mol Ł$^{-1}$ HCl by hydrothemal at 180 ℃ for 3 h, the porosity was distributed evenly and the pore size was decreased which all were beneficial to get a superior properties for the devices. In addition, the surface of the sample 1HM was rugged, and the thickness reached to about 10 ± 0.5 μm which was thinner than that of CM, as shown in Fig.2(b) and (b1). When the HCl concentration continued to increase, the thickness of the film was reduced furtherly to about 8 ± 0.5 μm and 4.5 ± 0.5 μm for 2HM and 4HM sample respectivly, as shown in Fig.2(c) and Fig.2(d). The mesoporous in the films became smaller and denser after the treatment. As a result, some relatively compact and a thinner films with the well-proportioned

distributed mesoporous structure had been obtained by the hydrothemal treatment.

In most time, TiO_2 showed an excellent chemical stability in the acidic condition which did't mean it was insoluble in acid. When the condiction was changed, the reaction was possible, especially in the condition of high temperature and pressure which had been proved in many articles.[31-33] In the study, the surface layer of the nanoporous TiO_2 film was first of all dissolved in the HCl solution slightly when the reaction kinetics was enhenced in the hydrothermal condition. And then, the Ti^{4+} ions began to recrystallize to generate TiO_2 and attach to the surface of the membrane with the increasing of ions concentration in solution. However, the fully recrystallization was impossible, and partical Ti^{4+} ions were still existed in solution. So, a thinner and more dense films with the mesoporous structure were obtained after the treatment. What's more, the film was dissolved more seriously when the HCl concentration increased. As a result, the sample 4HM showed the thinnest and densest film structure.

3.2 Photovoltaic properties analysis of TiO_2 films

Fig.3(a) shows the J-V curves of different electrodes under AM1.5 (100 mW cm^{-2}) illumination, and the corresponding parameters were listed in Table.1. The CM exhibited a conversion efficiency of 6.58 %, J_{sc} of 12.51 mA cm^{-2} and V_{oc} of 0.74 V. When the HCl concentration was lower than 4 mol L^{-1}, both the J_{sc} and V_{oc} of the treated samples were higher than that of CM, whereas the lower J_{sc} (10.90 mA cm^{-2}) was measured for the sample 4HM. And the DSSCs fabricated from the sample 1HM exhibited a PCE as high as 7.77 %, which was 18 % above the efficiency than the control film. But, the fill factor (FF) of the HCl treated samples was decreased when compared with CM sample. It was likely to be because that the redox transfer was affected by the decreased pore size.

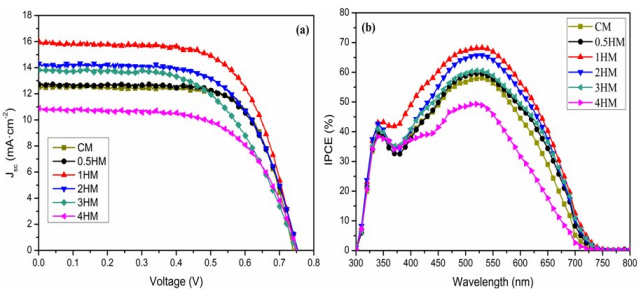

Fig.3 (a) J-V curves and (b) IPCE spectra of the DSSCs based on different TiO_2 films

Table.1 Photovoltaic properties and band gap value of the DSSCs based on different TiO_2 films

Electrodes	J_{sc} (mA cm^{-2})	V_{oc} (V)	FF (%)	H (%)	E_g (eV)
CM	12.51	0.74	71.1	6.58	3.18
0.5HM	12.73	0.75	68.01	6.51	3.12
1HM	16.04	0.75	65.12	7.77	3.11
2HM	14.37	0.75	62.93	6.77	3.10
3HM	13.81	0.75	58.17	6.01	3.10
4HM	10.90	0.75	62.50	5.11	3.04

Fig.3(b) shows the IPCE spectra of DSSCs based on different TiO_2 films. The IPCE values was enhanced when the photoanodes were treated by HCl. The DSSC based on 1 mol L^{-1} HCl hydrothermal treatment exhibited the best performance in the wavelength of 300-800 nm and reached the highest IPCE value at about 530 nm.

As shown in Fig.4, the electron life time was confirmed by the open circuit voltage decay (OCVD) measurement, which related to the electron transfer process in DSSCs.[34] It was well-known that the rate of open-circuit voltage decay was inversely proportional to the electron life time which can be calculated from OCVD curve by eq (1).[35]

$$\tau_n = -\frac{K_B T}{e}\left(\frac{dV_{oc}}{dt}\right)^{-1} \quad (1)$$

where

K_B is the Boltzmann constant

T is the absolute temperature

e is the electronic charge

It can be observed that the electron life time of the treated electrodes was longer than that of the control film at any V_{oc} value from 0-0.8 V. And the DSSC based on 1 mol L^{-1} HCl hydrothermal treatment electrode exhibited the longest electron life time when the four treated electrodes were compared. So, the electron recombination rate based on HCl hydrothermal treated electrode was lower and the electron transfer was more efficient. They leaded to the increased electron collection efficiency which would contribute to the improvement of the J_{sc}. The improvement of electron transfer efficiency may result from the shorter electron transfer pathway and higher crystallinity.

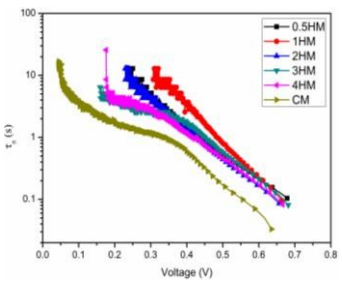

Fig.4 The OCVD curve of DSSCs based on different TiO_2 electrodes

3.3 Energy band analysis of TiO_2 films

To investigate the optical properties of different TiO_2 films, the UV-vis spectra over the wavelength range from 250 to 800 nm was performed. The band gap energy can be estimated by eq (2) for a direct band gap semiconductor.[36]

$$(\alpha h\upsilon)^{1/2} = k(h\upsilon - E_g) \quad (2)$$

Where

α is the absorption coefficient

E_g is the band gap

K is a constant

The estimated band gap can be confirmed by intercepting the tangent to the plot of $(\alpha h\upsilon)^{1/2}$ versus photon energy ($h\upsilon$) straight part. From the Fig.5(a), it can be observed that the treated electrodes exhibited red shift and the band gap decreased when compared to the control film. From the Table.1, it can be seen that

the band gap of the control film was 3.18 eV. The films with HCl hydrothermal treatment exhibited a lower band gap value from 3.12 to 3.04 eV. It indicated that the conduction band (CB) shifted positively and then the driving force of electron injection was increased in the DSSCs, resulting in the improvement of the electron injection efficiency from the LUMO of N719 dye to the CB of TiO_2. As reported, the Mott-Schottky plots of the films were measured to investigate the changes in the flat band potential (E_{fb}) of the electrode films.[37] The E_{fb} of the semiconductor film was associated with the space charge layer capacitance (C_{sc}) at semiconductor/electrolyte interface, and the relationship can be expressed using the eq (3).[38]

$$(C_{SC})^{-2} = 2(E - E_{fb} - K_B T/e)/N_D \varepsilon \varepsilon_0 e A^2 \quad (3)$$

where

E is the electrode potential
ε is the relative dielectric constant
A is the active surface
T is the absolute temperature
K_B is the Boltzmann constant

As shown in Fig.5(b), the E_{fb} of the CM sample was -0.49 V (vs SCE), whereas the E_{fb} of the treated electrode (1HM) was -0.37 V (vs SCE). It also corroborated that the conduction band could shift toward positive after the hydrothermal treatment to improve the electron injection efficiency, which would contribute to increase J_{sc} values. Furthermore, the reduced electron recombination implied a higher electron density which also benefited from the increased electron injection efficiency. And the V_{oc} in DSSCs highly depended on the electron density at the TiO_2 conduction band. As a result, the performace of the cells were better for the higher electron density after the treatment.

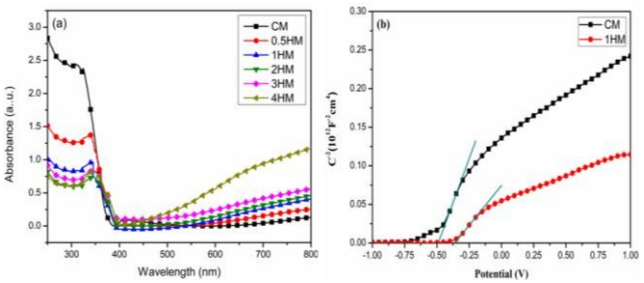

Fig.5 (a) Uv-vis diffuse reflectance spectra of the electrodes without loading N719 dye; (b) Mott-Schottky plots for the CM and 1HM samples

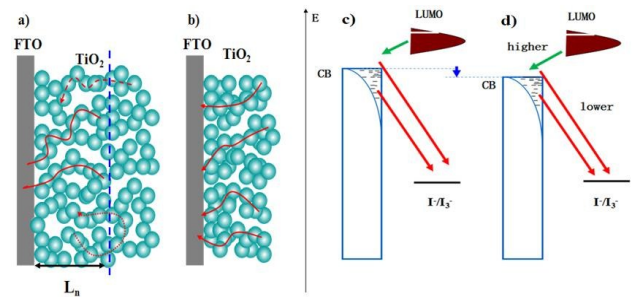

Fig.6 (a) and (b) is the schematic model of electron transfer processes; (c) and (d) is the schematic model of TiO_2 CB level alteration and recombination processes; (a) and (c) are the CM sample; (b) and (d) are the HM sample; L_n is the electron effective diffusion length

The Fig.6 shows the schematic model of electron transfer progress, the effect of HCl hydrothermal treatment on the TiO_2 conduction band level, and the recombination processes in the different films. In Fig.6(a) and (b), the solid line sugessted the effective electron transfer pathway. The electron over the L_n thickness in photoanode had no chance to transfer to FTO substrate.[39] The package between the nanoparticles lengthened the electron pathway which would lead to a increased electron recombination rate. After the HCl hydrothermal treatment and sintering (see Fig.6(b)), the thickness of the films decreased and the particles distribution was uniform. The increased connection and well-distributed particles indicated the TiO_2 internetworks may be more fully interconnected with other particles, which was beneficial for lessening the electron recombination rate and more electron may be collected at the FTO substrate. So, it was obvious that the electron life time of the treated electrodes was prolonged when compared to that of the control film. In Fig.6(c) and (d), the decreased TiO_2 conductive band level resulted in the improvement of driving force from N719 LUMO and a higher electron injection efficiency. Meanwhile, it was also beneficial for the reduction in electron recombination rate.

4. Conclusions

The TiO_2 films were treated with different concentrations of HCl by the hydrothermal method. The structure of the films were reformed, and the thickness of them were decreased after the hydrothemal treatment. A relatively compact and thinner films with the well-proportioned distributed mesoporous structure had been obtained in the study.The results showed the band gap of the treated electrodes was decreased with the improvement of HCl concentrations. The reduced recombination rate and enhancive electron injection efficiency contributed to the improvement of the J_{sc} and V_{oc}. The film treated with 1 mol L^{-1} HCl at 180 ℃ for 3 h showed the optimum PCE of 7.77% and J_{sc} of 16.04 mA cm^{-2}. This finding demonstrated the feasibility of HCl hydrothermal treatment TiO_2 in Dye-sensitized Solar Cells. What's more, it provided an effective way to reform the nanostructure of TiO_2 film to obtain a higher efficiency.

Acknowledgements

We thank the Key Laboratory of Oil and Gas Fields in Sichuan Universities and Colleges (Grant No. X151515KCL42) for financial support.

Notes and references

School of Materials Science and Engineering, Southwest Petroleum University, Chengdu 610500, PR China. Tel: +86 13550396098; Fax: +86 0288 3033286. Email: zj-656@163.com (J. Zhuang)

1. B. O'regan and M. Grätzel, *Nature*, 1991, **353**, 737-740.
2. B. E. Hardin, H. J. Snaith and M. D. McGehee, *Nat. Photonics*, 2012, **6**, 162-169.
3. M. Ye, D. Zheng, M. Lv, C. Chen, C. Lin and Z. Lin, *Adv. Mater.*, 2013, **25**, 3039-3044.
4. H. Abdullah, M. Z. Razali, S. Shaari and M. R. Taha, *Electron. Mater. Lett.*, 2014, **10**, 611-619.

5. M. Ye, J. Gong, Y. Lai, C. Lin and Z. Lin, *J. Am. Chen. Soc.*, 2012, **134**, 15720-15723.
6. D. GÜLtekin, M. Alaf and H. Akbulut, *Acta Phys. Pol. A*, 2014, **125**, 301-303.
7. Q. Wen, J. Zhuang, Q. He, Y. Deng, H. Li and J. Guo, *RSC Adv*., 2015, **5**, 91997 – 92003.
8. J. Qian, P. Liu, Y. Xiao, Y. Jiang, Y. Cao, X. Ai and H. Yang, *Adv. Mater.*, 2009, **21**, 3663-3667.
9. B. Tan, E. Toman, Y. Li and Y. Wu, *J. Am. Chem. Soc.*, 2007, **129**, 4162-4163.
10. S. Yang, H. Kou, J. Wang, H. Xue and H. Han, *J. Phys. Chem. C*, 2010, **114**, 4245-4249.
11. M. Wang, J. Ioccozia, L. Sun, C. Lin and Z. Lin, *Energ. Environ. Sci*., 2014, **7**, 2182-2202.
12. M. Quintana, T. Edvinsson, A. Hagfeldt and G. Boschloo, *J. Phys. Chem. C*, 2007, **111**, 1035-1041.
13. Z. S. Wang, Y. Cui, K. Hara, Y. Dan-oh, C. Kasada, A. Shinpo, *Adv. Mater.*, 2007, **19**, 1138-1141.
14. H. Horiuchi, R. Katoh, K. Hara, M. Yanagida, S. Murata, H. Arakawa and M. Tachiya, *J. Phys. Chem. B*, 2003, **107**, 2570-2574.
15. H. Yu, S. Zhang, H. Zhao, B. Xue, P. Liu and G. Will, *J. Phys. Chem. C*, 2009, **113**, 16277-16282.
16. B. C. O'Regan, J. R. Durrant, P. M. Sommeling and N. Bakker, *J. Phys. Chem. C*, 2007, **111**, 14001-14010.
17. O'. Brian, X. Li and G. Tarek, *Energ. Environ. Sci.*, 2012, **5**, 7203-7215.
18. Q. P. Liu, H. J. Huang, Y. Zhou, Y. D. Duan, Q. W. Sun and Y. Lin, *Acta Phys-Chim. Sin.*, 2012, **28**, 591-595.
19. Y. J. Shin, J. H. Lee, J. H. Park and N. G. Park, *Chem. Lett.*, 2007, **36**, 1506-1507.
20. S. Lee, J. Y. Kim, S. H. Youn, M. Park, K. S. Hong, H. S. Jung, J. K. Lee and H. Shin, *Langmuir*, 2007, **23**, 11907-11910.
21. J. Kim and J. Kim, *J. Nanosci. Nanotechno.*, 2011, **1**1, 7335-7338.
22. K. H. Park, E. M. Jin, H. Gu, S. Yoon, E. Han and J. Yun, *Appl. Phys. Lett*., 2010, **97**, 023302-023302-3.
23. H. Yu, B. Xue, P. Liu, J. Qiu, W. Wen, S. Zhang and H. Zhao, *ACS Appli. Mater. Inter.*, 2012, **4**, 1289-1294.
24. R. Gao, L. Wang, B. Ma, C. Zhan and Y. Qiu, *Langmuir*, 2009, **26**, 2460-2465.
25. Z. S. Wang, T. Yamaguchi, H. Sugihara and H. Arakawa, *Langmuir*, 2005, **21**, 4272-4276.
26. J. Singh, A. Gusain, V. Saxena, A. K. Chauhan, P. Veerender, S. P. Koiry, P. Jha, A. Jain, D. K. Aswal and S. K. Gupta, *J. Phys. Chem. C*, 2013, **117**, 2109 6-21104.
27. G. H. Guai, Q. L. Song, Z. S. Lu, C. M. Ng and C. M. Li, *Renew. Energ.*, 2013, **51**, 29-35.
28. S. Hao, J. Wu, L. Fan, Y. Huang, J. Lin and Y. Wei, *Sol. Energy*, 2004, **76**, 745-750.
29. K. H. Park, E. M. Jin, H. B. Gu, S. E. Shim and C. K. Hong, *Mater. Lett.*, 2009, **63**, 2208-2211.
30. A. Subramanian and H. W. Wang, *Appl. Surf. Sci.*, 2012, **258**, 7833-7838.
31. S. Dai, Y. Wu, T. Sakai, Z. Du, H. Sakai and M. Abe, *Nanoscale Res. Lett.*, 2010, **5**, 1829–1835.
32. E. Bright and D. W. Readey, *J. Am. Ceram. Soc.*,1987, **70**: 900-906.
33. Q. Huang, G. Zhou, L. Fang, L. Hu and Z. Wang, *Energy Environ. Sci*., 2011, **4**, 2145-2151.
34. G. K. Mor, K. Shankar, M. Paulose, O. K. Varghese and C. A. Grimes, *Nano Lett.*, 2006, **6**, 215-218.
35. A. Zaban, M. Greenshtein and J. Bisquert, *ChemPhysChem*, 2003, **4**, 859-864.
36. J. Liu, Y. Zhao, L. Shi, S. Yuan, J. Fang, Z. Wang and M. Zhang, *ACS Appl. Mater. Inter.*, 2011, **3**, 1261-1268.
37. F. Fabregat-Santiago, G. Garcia-Belmonte, J. Bisquert, P. Bogdanoff and A. Zaban, *J. Electrochem. Soc.*, 2003, **150**, E293-E298.
38. Q. P. Liu, H. J. Huang, Y. Zhou, Y. D. Duan, Q. W. Sun, Y. Lin, *Acta Phys. Chim. Sin.*, 2012, **28**, 591-595.
39. Q. Wang, J. E. Moser, M. Grätzel, *J. Phys. Chem. B*, 2005, **109**, 14945-14953.

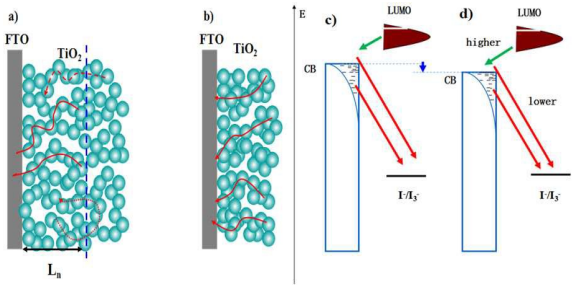

The thickness, band gap, and electron transfer of nanoporous TiO_2 film had been changed when it was treated by HCl.